ELSEVIER

Applied Surface Science 106 (1996) 80–89

applied surface science

Effect of lateral repulsion on desorption and diffusion kinetics SHG experiments and MC simulations

Zhao Wei [a], R. Verhoef [a], M. Asscher [a,*], I. Farbman [b], A. Ben-Shaul [b]

[a] *Department of Physical Chemistry and the Farkas Center for Light Induced Processes, the Hebrew University, Jerusalem 91904, Israel*
[b] *Department of Physical Chemistry and the Fritz Haber Center for Reaction Dynamics, the Hebrew University, Jerusalem 91904, Israel*

Received 17 September 1995; accepted 29 October 1995

Abstract

Activation energies for desorption and for diffusion were experimentally determined as a function of surface coverage for the system of ammonia on Re(001) utilizing optical second harmonic generation techniques. For the first time coverage grating with up to 5th order SH-diffraction is reported for K atoms on Re(001). Preliminary diffusion measurements were performed on this system as well. These systems may be considered as ideal model to study the effect of very strong lateral repulsion on the kinetics of desorption and diffusion. A MC study on the ammonia–Re(001) system is presented, which examines the significance of long range repulsive dipole–dipole interactions on the outcome desorption and diffusion kinetics. We found that a single set of parameters, within the dipole–dipole like $(1/r^3)$ dependence on adsorbates separation distance, explains qualitatively and in certain cases quantitatively the experimental observations. Interaction range up to 4th order neighbors must be computed in order to properly account for the results.

1. Introduction

The role of lateral interactions between neighbor adsorbates in affecting the kinetics of primary surface processes has long been recognized. Adsorbate aggregation, island formation, the appearance of different overlayer structures and phase transitions are among the surface phenomena which demonstrate the importance of adsorbate lateral interactions. All of these affect the local environment of the adsorbed particles and are thus expected to significantly affect the kinetics of the various surface processes such as diffusion, desorption, adsorption or chemical reaction.

Each of the above kinetic surface processes has been considered in details separately both experimentally and theoretically [1–5]. Quite often in these studies the effects of adsorbate lateral interactions are modeled in an approximate, mean field like, fashion. This approach is usually accurate only in the limit of low coverage or weak interactions. In case of strong interactions or high coverages, the interpretation of both theoretical and experimental (e.g. TPD) results becomes problematic.

The difficulties in the interpretation of experimental results (arising for example from compensation effect in desorption kinetics [6,7]) inspired the development of various theoretical approaches, including Monte-Carlo (MC) simulation schemes and a variety of mean field approximations, all aiming to account for the role of coverage on the rate of desorption. These calculations have revealed that the influence

* Corresponding author. Tel.: +972-2-6585742; fax: +972-2-618033; e-mail: asscher@batata.fh.huji.ac.il.

PII S0169-4332(96)00371-6

of lateral adsorbate interactions are often crucial and, moreover, that in general they can not be fully accounted for using simple coverage dependent rate parameters [8–12].

In recent years experimental studies of chemical diffusion on surfaces have become more accurate and accessible for a larger variety of molecular adsorbates, due to the introduction of laser desorption and diffraction techniques [4,13–19]. Using these methods, coverage effects on diffusion rates in systems governed by strong lateral interactions can be studied [20–24].

It is surprising to note that only few theoretical studies have addressed the effects of neighbor adsorbates simultaneously on these two, related, surface phenomena based on *the same theoretical model* [8,25]. Moreover, in most of the MC [26–30] or mean-field studies the interaction potentials between neighbor adsorbates are treated as adjustable parameters, chosen to fit either structural or kinetic data. Only rarely in these studies a physical (e.g. electrostatic) model is employed to derive their functional form [31].

In this paper we present experimental data on desorption (NH_3/Re(001)) and on diffusion (NH_3/Re(001) and K/Re(001)). For the desorption and diffusion of ammonia we present also MC simulations, attempting to scrutinize the role of adsorbate repulsive interactions on *both* the desorption and diffusion rates. The calculations attempt to explain some of the experimental data obtained for NH_3 adsorbed on Re(001) utilizing optical second harmonic generation (SHG) [24,32,33]. For this system, the isosteric heat of adsorption, the pre-exponential factor in the desorption rate constant and the diffusion coefficient were all determined as a function of coverage. In our theoretical treatment of this system we shall use a physically meaningful, long range dipole–dipole interaction potential, to account for the repulsive interactions between the adsorbed ammonia molecules.

2. Experimental results

The experimental set-up was described in detail in a previous publication [24]. Briefly, a UHV chamber equipped with sputter gun, quadrupole mass spectrometer for TPD and a Kelvin probe for work function measurements is running at a base pressure of 2×10^{-10} Torr. The Re(001) sample is mounted on a liquid nitrogen dewar with computer controlled temperature sweep (for TPD) or stabilization in the range 85–1600 K. Two p-polarized Nd:YAG lasers were used, one for generating adsorbate coverage grating via laser induced desorption (LID) and the second to obtain second harmonic generation (SHG) signals and SH-diffraction. For LID absorbed power densities at the crystal of the order of (5 ± 1) MW/cm^2 (non focused laser at approximately 80 mJ/pulse, after taking into account 75% reflectivity at 1064 nm) were sufficient to form rather deep modulation level in the case of ammonia monolayer coverage. In the case of potassium, however, due to stronger binding energy to the substrate and extremely strong coverage effect on the desorption rate,

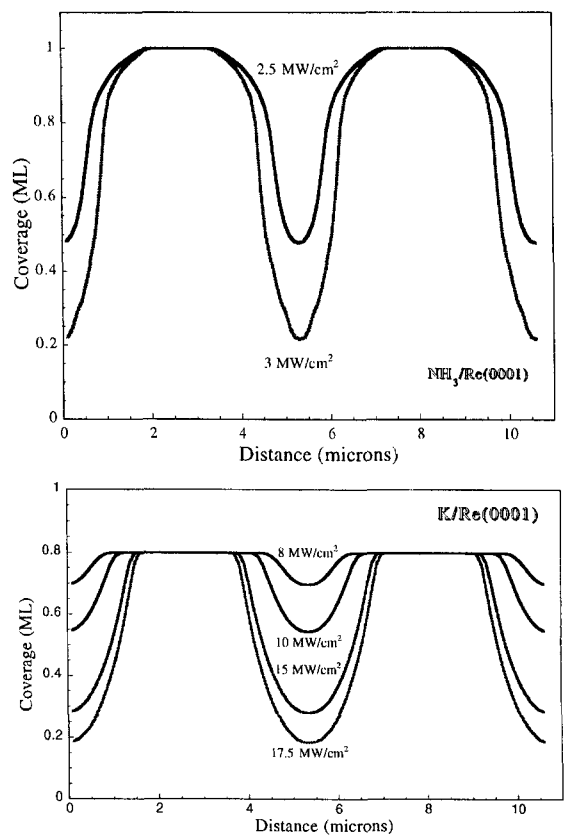

Fig. 1. Simulated coverage grating of potassium on Re(001) for different laser powers and different initial coverages.

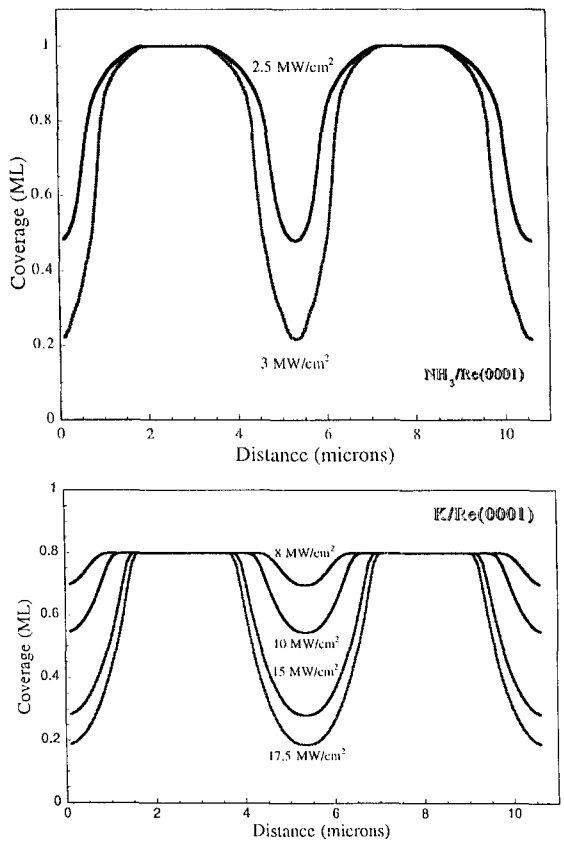

Fig. 2. A comparison of simulated grating formation with ammonia and with potassium on Re(001).

higher power densities of 10–15 MW/cm^2 were required for coverages of the order of 0.6–1.0 ML.

The experimental data for the desorption parameters as a function of coverage [33], laser induced desorption [32] and diffusion measurements [24] of ammonia on Re(001) were all presented previously. Here, we shall present only the results concerning the grating formation and preliminary diffusion measurements of potassium on Re(001). These are the first measurements for alkali atoms on any metal substrate, using the above optical techniques. The diffusion of K on Ru(001) was investigated recently using the LID hole-refilling technique [20b].

A necessary requirement for the analysis of coverage grating formation of an adsorbate on metal surfaces is the knowledge of its desorption kinetic parameters as a function of coverage. This information allows one to simulate the laser induced desorption (LID) process which produces the coverage grating [32,21,24]. This is particularly important in the case of alkali atoms since their desorption kinetics varies dramatically with coverage because of repulsion among neighbor atoms.

In Fig. 1, a simulation of the coverage grating of potassium on Re(001) is presented for different laser power densities and initial coverages. The different shapes of the coverage modulations reflect the extremely strong effect of coverage on the desorption rate. Comparison of the modulation shapes as a result of the specific interatomic or intermolecular interactions for two different adsorbates reveals the importance of lateral interactions on the grating formation process. This is demonstrated for ammonia and potassium on Re(001) in Fig. 2.

The experimental manifestation of the formation of a monolayer grating is obtained if SHG diffraction

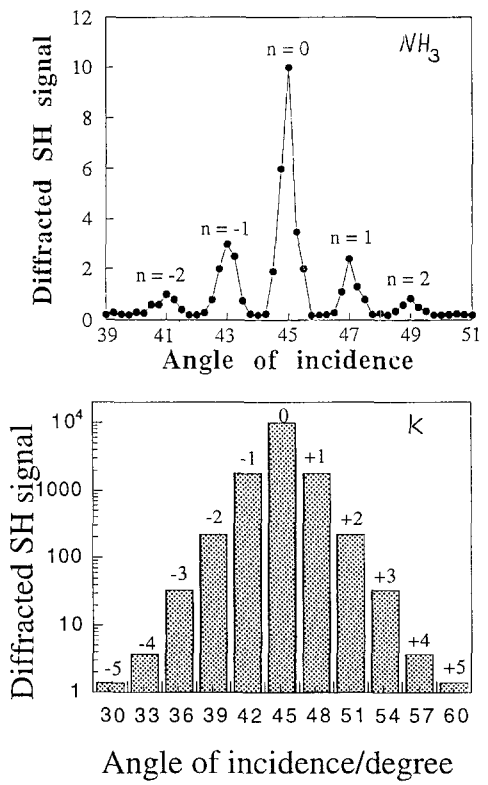

Fig. 3. Diffracted SH signal from ammonia and potassium monolayer gratings. Initial coverage is 1 ML, grating formation laser power density is 12 MW/cm^2 for potassium and 3 MW/cm^2 ammonia.

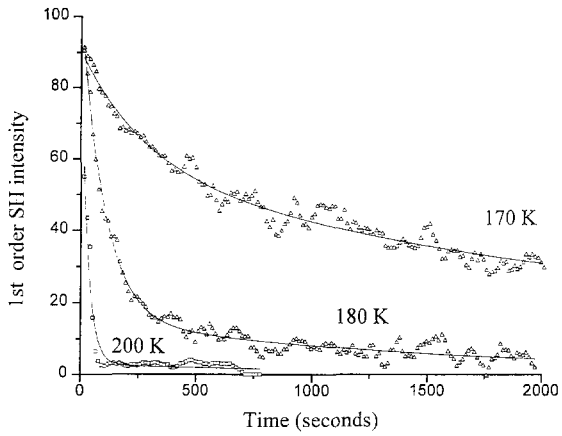

Fig. 4. Decay of first order SH-diffraction peak as a function of time at several crystal temperatures, reflecting direct monitor of surface diffusion. System is K on Re(001).

signal is observed while changing the sample angle with respect to the photomultiplier detector. Diffraction signals from ammonia and potassium gratings are shown in Fig. 3. In principle, reversed Fourier analysis based on the relative diffracted intensities of the different orders should enable to reconstruct the actual coverage modulation and can be compared with the simulated shapes such as those in Fig. 2. Finally, in order to directly follow surface diffusion, the decay of the first or higher order diffraction peaks with time at different crystal temperatures is recorded. An example is shown in Fig. 4 for the decay of the first order diffraction peak following grating formation of K on Re(001).

Microscopic understanding of the data obtained for desorption kinetics and for diffusion is difficult mostly because of lateral interactions among neighbors. The local variation in the number of neighbors and the different separation distances between them require careful simulation of the meaning of the actual kinetics which is measured. This can be achieved by the employment of Monte-Carlo simulations. Below we present a model which attempts to explain the experimental results for ammonia desorption and diffusion on Re(001). It is assumed that the same type of interaction dictates both desorption and diffusion. The model is based on uniform physical origin for the repulsive interaction between neighbors, namely dipole–dipole like interaction. This means that each neighbor molecule will affect the barrier for desorption and for diffusion by an amount which decreases with the separation distance r as C/r^3.

3. Monte-Carlo simulations

3.1. Energetics

We model the Re(001) surface as a perfect hexagonal lattice of adsorption sites, consistent with the assumption that the ammonia molecules adsorb uniformly at either on-top or three fold hollow sites. The exact position of the adsorption site has not been determined experimentally. The simulations were performed on two-dimensional (2D) hexagonal lattices comprising 60×60 sites, with periodic boundary conditions. Test simulations on larger lattices (84×84 sites) were performed in order to asses the importance of finite size effects, revealing that for the systems studied in this work these effects are negligible. This is consistent with the work of Sandhoff et al. [34], who found a lattice of 60×60 sites to give most satisfactory results for a similar system.

Experimentally, the saturation coverage in the NH_3/Re system is $\theta_s = 0.25$, indicating that the ammonia molecules can not occupy nearest-neighbor (NN) sites due to very strong (electrostatic and/or excluded volume) repulsive forces [33]. Consequently, the distance of closest approach in our simulations was set to $r_0 = 2$, in units of the lattice constant. Hereafter, coverages, θ, will be taken relative to the saturation coverage.

The experimental data suggest that the lateral interactions between the adsorbed ammonia molecules are repulsive [11,28,36]. We assume that they are pairwise additive and model them using a dipole–dipole interaction potential of the form

$$U_{ij} = \begin{cases} U_0/r_{ij}^3 & \text{if } r_{ij} \le r^*, \\ 0 & \text{if } r_{ij} > r^*, \end{cases} \quad (1)$$

with r_{ij} denoting the distance between sites i and j, and r^* is a 'cut-off' radius (see below), both measured in units of r_0. The interaction potential U_0 between two adsorbates at distance r_0, was set to 2 kcal/mol in all the calculations reported below. This value corresponds, for example, to the repulsive

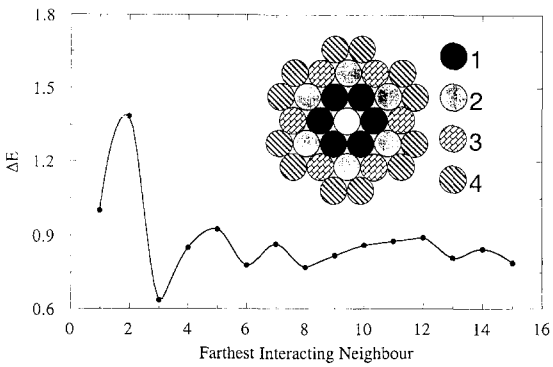

Fig. 5. The energy change, ΔE, associated with perturbing a perfect (2×2) layer by moving one particle to a nearest neighbor vacant site. The perturbation energy is shown as a function of the range r^*, of the repulsive dipole–dipole potential (see Eq. (1)). For convenience the abscissa is expressed in terms of the 'farthest neighbor' included in the range of interaction. In units of the lattice constant $r^*/r_0 = 1, \sqrt{3}, 2, \sqrt{7}, \ldots$ correspond here to farthest neighbor 1, 2, 3, 4,..., respectively, see insert. Energy is given in units of nearest-neighbor interaction.

interaction between two parallel dipoles of 2 D (the dipole moment of ammonia on Re(001) as determined by work function measurements [35]) at a distance of 3.0 Å from each other. The cut-off distance r^* is introduced in order to keep the calculations tractable. It is supposed to represent the distance beyond which adsorbate–adsorbate interactions do not affect significantly the kinetic and structural characteristics of the adlayer. To obtain a reasonable estimate of this distance we have considered a perfectly ordered 2×2 adlayer, and, using Eq. (1), calculated the energy change ΔE associated with moving one of the adsorbed particles into a NN site (thus creating an isolated defect), as a function of r^*. The results of this calculation are shown in Fig. 5 together with definition of the interaction ranges. Noting that ΔE does not vary significantly once $r^*/r_0 \geq \sqrt{7}$ we have set $r^*/r_0 = \sqrt{7}$ as the 'standard' (or 'full') interaction range in our calculations. For the sake of comparison, and for demonstrating the importance of the range of interaction in modeling surface kinetic phenomena we have also carried out some calculations for a shorter cut-off distance, namely $r^*/r_0 = \sqrt{3}$. Note that $\sqrt{7}$ and $\sqrt{3}$ correspond, on the triangular lattice, to the distance between 4th-order and 2nd-order neighbors, respectively.

The model described above was used to study, theoretically, the kinetics of particle diffusion and desorption as a function of coverage and temperature. The temperature range considered was 40 K to 240 K, which includes both the temperature range of diffusion measurements (105–130 K) and equilibrium–desorption experiments (160–240 K) of the NH_3/Re system [24,33]. The diffusion and desorption experiments were modeled using standard Monte Carlo (MC) simulations.

3.2. Isosteric heat of adsorption

The adsorption–desorption experiments which motivated the present study were performed under equilibrium conditions [32,33]. Namely, the adsorbed layer has been brought to equilibrium, at different coverages and temperatures, with the molecules at the gas phase. To ensure similar conditions in our MC simulations we have first randomly populated the lattice sites according to the prescribed value of θ, and then performed particle moves with acceptance criteria according to the usual Metropolis scheme. To enhance the equilibration process no restrictions were set on the range of particle displacements. In fact, the simulation procedure employed is equivalent to a sequence of particle desorption–adsorption events weighted, as usual, by the local interaction energies in the old and new sites.

Experimentally, the sticking coefficient of NH_3 on Re(001) is 1, independent of coverage, implying zero activation energy for adsorption [33]. Consequently, the activation energy for desorption is equal to the isosteric heat of adsorption, which can be computed as follows [36]:

$$\Delta H = -\partial\beta\mu/\partial\beta. \tag{2}$$

Here ΔH is the adsorption enthalpy (or activation energy for desorption), μ is the chemical potential of the system and $\beta = 1/kT$, with k denoting Boltzmann's constant and T the absolute temperature.

The chemical potential was calculated, as common in canonical MC simulations, using the (Widom's) 'insertion' formula [37],

$$\beta\mu = \ln\theta - \ln\{\exp(-\beta\varphi)\}. \tag{3}$$

Here φ is the potential energy increment associated

with the insertion of a particle into a randomly chosen lattice site (being infinite for occupied sites).

3.3. Diffusion kinetics

The chemical diffusion coefficient D was calculated using the expression [4,28]

$$D = (1/4t)PC, \tag{4}$$

where t is the time, and P and C denote, respectively, the 'thermodynamic factor' and the 'time correlation function'. The thermodynamic factor is given by

$$P = \partial\beta\mu/\partial \ln \theta = \langle N\rangle/\langle(\delta N)^2\rangle, \tag{5}$$

where $\langle N\rangle$ is the average number of adsorbed particles and $\langle(\delta N)^2\rangle$ is the fluctuation in N.

The factor C is proportional to the time correlation function of the motion of the center of mass of the system. It is given by [4,28]:

$$C = (1/N)\langle|\sum[r_i(t) - r_i(0)]|^2\rangle, \tag{6}$$

where $r_i(t)$ is the position of particle i at time t. The summation extends over all particles.

The derivation of Eq. (4) is discussed in detail elsewhere [4]. Qualitatively, the appearance of the thermodynamic factor in D derives from the fact that the driving force for particle diffusion are local density gradients. When the thermodynamic equilibrium state itself is characterized by large density fluctuations, this driving force decreases.

Both the thermodynamic factor and the correlation function were calculated by performing MC simulations (of different kinds, see below) for systems in thermodynamic equilibrium. The thermodynamic factor can be calculated using either the first or the second equality in Eq. (5), namely, by calculating either $\partial\beta\mu/\partial \ln \theta$ or $\langle N\rangle/\langle(\delta N)^2\rangle$. The first route requires the calculation of $\beta\mu$ as a function of θ. This can be done using the particle insertion method, as mentioned with respect to Eq. (3). The second route involves grand-canonical simulations, i.e., simulations at constant μ, T and A, where A is the total area of the lattice. We have performed both types of calculations, finding generally excellent agreement between them.

The correlation function C was calculated by means of kinetic MC simulations. Basically, the procedure adopted is to follow many particle 'trajectories' $r(t)$ over long periods of time and use Eq. (6) to evaluate C. The trajectories were simulated as sequences of particle jumps between nearest-neighbor sites, with transition probabilities of the Arrhenius form. More explicitly, in these simulations a particle is randomly chosen and then allowed to hop into a randomly chosen neighboring site. If the new site is already occupied the move is rejected. Otherwise it is accepted, with probability $p = \exp(-\varepsilon_b/kT)$, where ε_b denotes the activation barrier for diffusion. As usual, one Monte-Carlo step (MCS) corresponds, by definition, to one attempted move per particle (on the average). A connection between the MC time and real time is established by identifying 1 MCS $= 1/\nu$ where ν is the experimental frequency of attempted jumps, which is, typically, in the range 10^{12}–10^{17} s^{-1}. In general ν is taken as the pre-exponential factor in the Arrhenius formula for the hopping rate of a single (non-interacting) particle on the surface. For the NH_3/Re system $\nu \approx 10^{15}$ s^{-1} at $\theta = 0.5$.

The activation barrier and hence the jump probability from one site to another depends on the local environments of both the initial and the final sites. Various expressions have been suggested to model the influence of adsorbate lateral interactions on the hopping rate (for a review see e.g. Ref. [10c]). We have utilized 'the intersecting harmonic wells (IHW) scheme' [10c]. In the IHW model ε_b (the barrier for diffusion) depends on the local environments of *both* the initial and the final sites (see below).

Each adsorption site is regarded as an harmonic potential well [10]. The intersection point of the potential wells corresponding to two neighboring sites i and j, is envisaged as a saddle point, see Fig. 6. The height of this saddle point, relative to the minimum of the potential well centered around site i, defines the barrier energy for the particle jump from site i to site j. The barrier height $\varepsilon_b(i \to j)$ depends on the local environments of both the initial and the final sites. It is easily verified that $\varepsilon_b(i \to j) - \varepsilon_b(j \to i) = \Delta\varepsilon(i \to j)$ is simply the energy difference between the bottoms of the potential wells corresponding to sites j and i. Hence the model satisfies detailed balancing. The dependence of $\Delta\varepsilon(i \to j)$ on the local environments of sites i and j follows from the fact that $\Delta\varepsilon(i \to j) = V(j) - V(i)$,

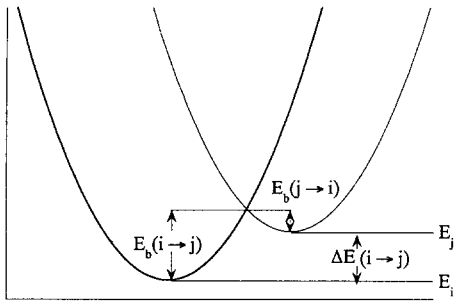

Fig. 6. A scheme of the intersecting harmonic well model for describing the diffusion barrier.

where $V(i, j)$ are the destabilization energies at sites i and j due to the presence of neighbors.

Explicitly, the height of the activation barrier for the $i \rightarrow j$ transition is given by

$$\varepsilon_b = \varepsilon_b\left[1 - \Delta\varepsilon(i \rightarrow j)/4\varepsilon_b^0\right]^2. \quad (7)$$

Here ε_b^0 is the barrier height for diffusion of an isolated particle or, in other words, the barrier to diffusion when $\theta \rightarrow 0$. In our calculations this quantity was taken from experiment [24], namely $\varepsilon_b^0 = 3.4$ kcal/mol.

4. Results and discussion

The range of lateral interactions plays a crucial role in determining the structure of the adsorbed layer, and hence in the kinetics of surface processes, especially at high coverages. While it is well known that the type and range of adsorbate lateral interactions play a prominent role in determining the phase behavior of adsorbed overlayers [35,38], the effects of these characteristics on the kinetics of surface processes has hardly been investigated. We have performed MC simulations using several different values of r^*/r_0, revealing qualitatively and quantitatively different results for both the desorption and the diffusion rates. The best (though nowhere perfect) agreement with experiment was found for the longest ('full') range of the interaction potential ($r^*/r_0 = \sqrt{7}$). Details on the interaction range aspect were given elsewhere [38].

The diffusion coefficient D is a product of two factors, the thermodynamic factor P and the time correlation function C, both depending sensitively on the adlayer structure. The thermodynamic factor is large whenever the fluctuations in N are small, as is the case when the system is fully ordered.

The thermodynamic factor P and the correlation function C were both calculated using our MC scheme taking into account the longest interaction range. It was found that C/t reaches minima at those coverages (of perfect long range order) where the thermodynamic factor is maximal. Not surprisingly, the diffusion coefficient, D, which is a product of P and C/t varies sensitively, seemingly erratically, with θ, as shown in Fig. 7. Taking into account the computational errors, we note that D is not a smooth function of θ, reflecting the transitions undergone by the adlayer between phases of different symmetries. Experimentally, due perhaps to kinetic effects (activation and nucleation barriers to phase transitions and the appearance of defects in and between the finite size domains of ordered structures) the diffusion coefficient varies more smoothly with coverage.

Whenever the adlayer is fully ordered any addition of particles into vacant 'interstitial' sites involves the creation of high energy defects. For instance, adding particles to the perfectly ordered ($\sqrt{3} \times \sqrt{3}$) layer of the $r^*/r_0 = \sqrt{7}$ system, results in the formation of several high energy NN contacts. Particle desorption from these ('defect') sites is easier than desorption from the ordered phase and we

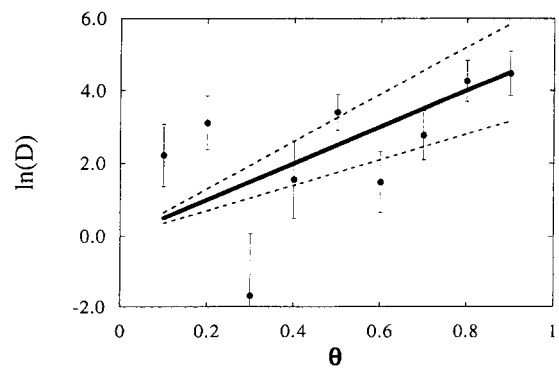

Fig. 7. The chemical diffusion coefficient D as a function of coverage, at $T = 120$ K. The experimental results [11,28] are shown as heavy solid line, with the dashed lines marking the uncertainty limits. The dots are the results of MC simulations ($r^*/r_0 = \sqrt{7}$).

expect a change in the slope of the activation energy for desorption around $\theta = 1/3$. Just above $\theta = 1/3$, the added particles can adsorb far apart from each other (even when randomly distributed among the available sites) thus avoiding repulsive interactions between them. At this coverage range we expect the desorption rate to change (decrease) rather slowly, since the desorbing particles are those adsorbed at the interstitial sites. The decrease of the activation energy for desorption with coverage is due to lateral interactions between these interstitial adsorbates. Eventually another ordered phase appears (e.g., the $\sqrt{3} \times \sqrt{3}$) structure of vacancies at $\theta = 2/3$) and the activation energy will again exhibit a sharp change with coverage. These qualitative trends are corroborated both experimentally and theoretically. More details in Ref. [38].

The coverage dependence of the activation energy for desorption, as obtained experimentally for the NH_3/Re(001) system, is shown in Fig. 8. Also shown in this figure are the results of our MC simulations. Both the experimental and the theoretical results show marked changes in slope at two intermediate coverages. In the simulations these changes take place at $\theta = 1/3$ and $2/3$, consistent with the qualitative analysis above. The experimental changes in slope occur at $\theta \approx 0.3$ and 0.75. Considering the complexity of the system investigated and the high sensitivity of the desorption rate to phase changes, as demonstrated in previous sections, we regard the comparison between theory and experiment as satisfactory. The quantitative agreement, at least with regards to the range of variation of the activation energy, is also reasonable. It should be added that the uncertainties in the experimental values corresponding to the limits of low and high coverage are considerable (± 2 kcal/mol).

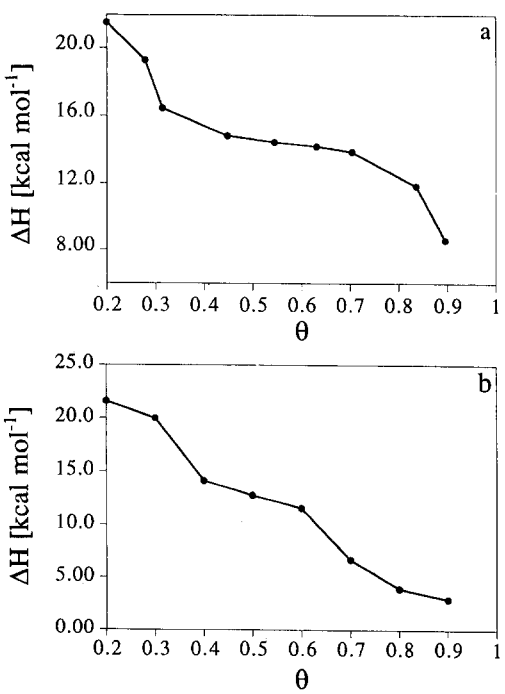

Fig. 8. Activation energy for desorption: (a) Experimental results; (b) Monte-Carlo simulations.

In Fig. 7, where we showed the calculated diffusion coefficient, we also show the $D(\theta)$ curve obtained experimentally for the NH_3/Re(001) system. The simulations involve considerable uncertainties due, mainly, to difficulties associated with the calculation of the correlation function C. These are reflected by the large error bars associated with the theoretical points in Fig. 7. The experiments also involve sizable uncertainties (± 1 in $\ln\{D\}$, which originates from ± 0.2 kcal/mol in activation energy), associated with the interpretation of the grating-diffusion measurements. Considering all these provisos, the agreement between experiment and theory shown in Fig. 7 should be regarded as reasonable.

In judging the agreement between experiment and theory it should be noted that we have used the same model, namely Eq. (1), to describe both the desorption and the diffusion experiments. The strength of the dipole–dipole like interaction potential was chosen to fit the desorption data, but no further adjustments were made to fit the diffusion measurements.

5. Conclusions

Optical second harmonic generation was utilized to study desorption (NH_3/Re(001) and diffusion (NH_3 and K on Re(001). For diffusion measurements laser induced desorption is used to generate coverage grating from which a second laser is used to generate SH-diffraction. The decay of the higher order diffraction signal at different crystal temperatures has been used to study the diffusion of potassium on Re(001) for the first time.

The dependencies on coverage of the activation energies corresponding to two very different surface processes, desorption and diffusion, were explained using one rather simple theoretical model. This model was applied to the system of ammonia on Re(001). The basic assumption of the model is that the lateral interactions between the adsorbed particles are repulsive and can be described by a dipole–dipole like interaction potential, with a rather long range of interaction.

We found that a kinetic model to diffusion in which the activation barrier depends on lateral interactions of the hopping particles in both the initial and final sites provides reasonable agreement with experimental results. The coverage dependencies of the activation energy for desorption, the thermodynamic factor, and the correlation function were all found to depend critically on the range of interaction. We found that a reasonable fit to the experimental data is obtained by setting the repulsion between nearest-neighbors at 2 kcal/mol. This value is 5.7 times larger than the repulsion between two ammonia dipoles at the minimum separation (assumed to be dictated by a (2×2) structure). This discrepancy has not been analyzed within the framework of this work and deserves further study.

Acknowledgements

This work was partially supported by a grant from the Israel Science Foundation and the US–Israel Binational Foundation. The Fritz Haber Research Center is supported by the Minerva Gesellschaft für die Forschung mbH, Munich, BRD. The Farkas Center for Light Induced Processes is supported by the Bundesministerium fur Forschung und Technologie and the Minerva Gesellschaft fur die Forschung mbH.

References

[1] D.P. Woodruff and T.A. Delchar, Modern Techniques of Surface Science, 2nd ed. (Cambridge University Press, 1994).
[2] J.T. Yates, Jr., in: Methods of Experimental Physics, Vol. 32, Solid State Physics – Surfaces, Eds. R.L. Park and M.G. Lagally (Academic Press, 1985) ch. 8.
[3] G. Ehrlich and K. Stolt, Annu. Rev. Phys. Chem. 31 (1980) 603.
[4] R. Gomer, Rep. Prog. Phys. 53 (1990) 917.
[5] J.K. Norskov, S. Holloway and N.D. Lang, J. Vac. Sci. Technol. A 3 (1985) 1668.
[6] P.J. Estrup, E.F. Greene, M.J. Cardillo and J.C. Tully, J. Phys. Chem. 90 (1986) 4099.
[7] J.L. Taylor and W.H. Weinberg, Surf. Sci. 78 (1978) 259.
[8] M. Silverberg and A. Ben-Shaul, J. Chem. Phys. 87 (1987) 3178; Surf. Sci. 214 (1989) 17.
[9] D.L. Adams, Surf. Sci. 42 (1974) 12.
[10] (a) E.S. Hood, B.H. Toby and W.H. Weinberg, Phys. Rev. Lett. 55 (1985) 2437; H.C. Kang and W.H. Weinberg, (b) Surf. Sci. 299/300 (1994) 755; (c) Acc. Chem. Res. 25 (1992) 253.
[11] V.P. Zhdanov, Surf. Sci. 137 (1984) 515.
[12] O.M. Becker, I. Chacham, M. Asscher and A. Ben-Shaul, J. Phys. Chem. 93 (1989) 8059.
[13] S.M. George, A.M. DeSantolo and R.B. Hall, Surf. Sci. 159 (1985) L425.
[14] C.H. Mak, J.L. Brand, A.A. Deckert and S.M. George, J. Chem. Phys. 85 (1986) 1676.
[15] E.G. Seebauer and L.D. Schmidt, Chem. Phys. Lett. 123 (1985) 129.
[16] X.D. Zhu, Th. Rasing and Y.R. Shen, Phys. Rev. Lett. 61 (1988) 2883.
[17] T. Suzuki and T.F. Heinz, Opt. Lett. 14 (1989) 1201.
[18] X.D. Zhu, A. Lee and A. Wong, Appl. Phys. A 52 (1991) 317.
[19] X.-D. Xiao, Y. Xie and Y.R. Shen, Surf. Sci. 271 (1992) 295.
[20] (a) A.A. Deckert, J.L. Brand, M.V. Arena and S.M. George, Surf. Sci. 208 (1989) 441; (b) E.D. Westre, D.E. Brown, J. Kutzner and S.M. George, Surf. Sci. 294 (1993) 185.
[21] X.-D. Xiao, X.D. Zhu, W. Daum and Y.R. Shen, Phys. Rev. B 46 (1992) 9732; B 48 (1993) 452.
[22] G.A. Reider, U. Hofer and T.F. Heinz, Phys. Rev. Lett. 66 (1991) 1994.
[23] X.D. Zhu, A. Lee, A. Wong and U. Linke, Phys. Rev. Lett. 68 (1992) 1862.
[24] Z. Rosenzweig, I. Farbman and M. Asscher, J. Chem. Phys. 98 (1993) 8277.
[25] B. Terreault, J. Appl. Phys. 62 (1987) 152.
[26] M. Bowker and D.A. King, Surf. Sci. 71 (1978) 583; 71 (1978) 208.
[27] M.C. Tringides and R. Gomer, Surf. Sci. 265 (1992) 283.
[28] C. Uebing and R. Gomer, J. Chem. Phys. 95 (1991) 7626.
[29] D.A. Reed and G. Ehrlich, Surf. Sci. 102 (1981) 588.
[30] S.-L. Lee, F.-Y. Li and C. Li, Chem. Phys. Lett. 168 (1990) 283.
[31] J.K. Norskov, in: The Chemical Physics of Solid Surfaces and Heterogeneous Catalysis, Vol. 6, Eds. D.A. King and D.P. Woodruff (Elsevier, Amsterdam, 1992).
[32] Z. Rosenzweig and M. Asscher, J. Chem. Phys. 96 (1992) 4040.
[33] Z. Rosenzweig and M. Asscher, Surf. Sci. 225 (1990) 249.
[34] M. Sandhoff, H. Pfnür and H.-U. Everts, Surf. Sci. 280 (1993) 185.
[35] M. Asscher, Proc. SPIE – Int. Soc. Opt. Eng. 2125 (1994) 19.

[36] M.P. Allen and D.J. Tildesley, in: Computer Simulation of Liquids (Oxford Science, 1992) pp. 49–50.
[37] J.S. Walker and M. Schick, Phys. Rev. B 20 (1979) 2088; K.A. Fichthorn, E. Gulari and R.M. Ziff, Surf. Sci. 243 (1991) 273; P Piercy, K. De'Bell and H. Pfnür, Phys. Rev. B 54 (1992) 1869; M. Sandhoff, H. Pfnür and H.-U. Everts, Europhys. Lett. 25 (1994) 105.
[38] I. Farbman, M Asscher and A. Ben-Shaul, J. Chem. Phys. 104 (1996) 5674.